Use of AI in Automated Billet Quality Assessment

Martijn Vos[1], Ivan Gerasimov[2], Tatiyana Kovaleva[3], Sorokin Evgeniy[4], Cherepanov Vyacheslav[5] and Losev Aleksey[6]
1. Director New Product Commercialization
RUSAL Aluminium Management, Moscow, Russia
2. Manager Aluminium Alloys Research Laboratory of SALC
3. Director Scientific & Analytical Laboratory Complex (SALC)
4. Director Department of Data Analysis Systems Development
5. Lead Specialist Department of Data Analysis Systems Development
6. Software Developer Department of Data Analysis Systems Development
RUSAL Engineering and Technology Center, Krasnoyarsk, Russia
Corresponding author: vos_martijn@yahoo.com
https://doi.org/10.71659/icsoba2025-ch007

Abstract

RUSAL, a leading global aluminium producer has revolutionized the microstructure analysis of aluminium ingots by implementing artificial intelligence (AI). Developed by RUSAL's Engineering and Technology Center, this AI-driven system utilizes machine vision and deep learning to assess billet quality, significantly reducing analysis time to just 15 minutes. This technology enhances quality control and minimizes manual tasks, ensuring durability and performance in industries such as construction, mechanical engineering, and aerospace.

The AI system evaluates cylindrical ingots, a high-demand aluminium product, across eight key microstructural parameters, including grain size and inclusions. Traditional analysis methods can take up to four hours, whereas the AI system delivers comprehensive reports rapidly. This advancement demonstrates the transformative impact of industrial AI on quality control processes.

Operational at the RUSAL Engineering Center laboratory, the technology is set to be deployed in aluminium smelter laboratories for real-time quality assessment. Each parameter is analysed by dedicated neural networks trained on annotated digital microscope images, achieving accuracy comparable to trained technicians while eliminating human error. This ensures consistent quality control and optimal material performance across various industries.

Keywords: Neural networks and deep learning, Microstructure analysis, Aluminium billet, Machine vision, Artificial intelligence and quality control.

1. Introduction

Extrusion billets made from 6xxx series alloys represent advanced, high-quality products in today's aluminium industry. Beyond essential factors like chemical composition, surface quality, geometry, and macrostructure, microstructure stands as a critical performance characteristic. Its quality directly affects extrudability, anodized surface quality, and the mechanical properties of the final profile. Specific, defined microstructural features distinguish high-quality billets from poor ones. The measurement and rating of these features form an established standard: the Billet Microstructure Quality Assessment.

1.1 Billet Microstructure Quality Assessment

The main controlled parameters of the microstructure are:

- Number and size of inclusions;
- Inverse segregation zone size;
- Grain size;
- Porosity volume fraction and size;
- Degree of transformation and fragmentation of AlFeSi-particles;
- Number of Mg_2Si particles;
- Distribution type of secondary Mg_2Si particles.

As shown in Table 1, each of the above parameters influences the extrusion process and the quality of the produced aluminium profiles.

Table 1. Microstructure parameters influence on extrusion process and product quality [1, 8, 11, 13-25].

Process	Microstructure parameter						
	Number and size of inclusions	Inverse segregation zone size	Grain size	Porosity volume fraction and size	Degree of transformation and fragmentation of AlFeSi-particles	Number of Mg_2Si particles	Distribution type of secondary Mg_2Si particles
Extrusion							
Extrusion speed	-	-	significant	-	severe	severe	severe
Pick-ups	some	-	-	-	severe	significant	-
Surface Roughness	severe	some	-	significant	significant	some	-
Die lines	significant	some	-	-	significant	-	-
Blisters	some	-	-	significant	-	-	-
Tearing	some	significant	-	-	significant	some	-
Die bearing condition	severe	some	-	-	significant	-	-
Weld seams and back-end defect	some	severe	-	-	-	-	-
Mechanical properties							
Tensile strength	some	-	some	-	-	severe	severe
Yield strength	some	-	some	-	-	severe	severe
Elongation	some	-	some	-	-	severe	severe
Hardness	some	-	some	-	-	severe	severe
Anodizing response							
Surface dullness	-	-	-	some	significant	severe	severe
Colour match	-	-	-	-	significant	severe	severe
Streaks	-	-	significant	-	-	-	-

Currently in RUSAL, microstructure control is performed either manually by laboratory technicians through the eyepieces of inverted optical microscopes or semi-automatically using image analysis software.

RUSAL has developed and uses the certified RAM-ST-2.6-25 method (certificate No. 221.0066/RA.RU.311866/2024) to analyse the microstructure of 6xxx series alloy extrusion billets. This methodology establishes the relationship between each analysed billet parameter and a specific production process, assesses the billet's potential extrudability during further processing, and evaluates its contribution to the final product's characteristics. A brief description of the approaches to analysing the main parameters of the microstructure of billets is provided below. Figure 1 shows a typical appearance of the analysed microstructure objects.
The quantity and size of non-metallic inclusions are primarily determined by the quality and technology of the billet casting process (i.e., refining, modification, and filtration). They begin to appear in the aluminium melt at the start of electrolysis [1]. The primary method for determining their quantity is the PoDFA method [1, 8]. However, when monitoring the microstructure, a metallographic analysis of a microsection taken from the slice is also performed. When analysing nonmetallic inclusions, the laboratory assistant sequentially scans a certain area of the microsection to detect and identify the inclusions. Then, the assistant determines their size using an ocular grid or tools for linear measurements from the image captured by the microscope camera. Various types of inclusions are found in billets: TiB_2, Al_4C_3, Al_2O_3, etc., which differ in appearance and origin. Typically, they are found in agglomerates. Figure 1(a) shows a typical type of inclusion in the microstructure.

The inverse segregation zone (ISZ) is a structural component of billet surface with a different chemical composition and structure than the main part of the metal [1]. It almost always occurs during casting with modern commercial casting systems. The thickness of the ISZ is determined during the billet casting process and is a consequence of the inverse liquation process. In other words, it characterizes the degree of surface liquation in the billet. The size of the ISZ is estimated by marking the boundary of the area with the highest concentration of alloying elements and phase particles near the surface (Figure 1b). Then, the depth of the zone is measured in several areas using an ocular grid or linear measurements in an image analysis software.

Grain formation occurs during billet crystallization, and grain size depends on modification and casting conditions. The production goal is to obtain a homogeneous, relatively small, equiaxed grain throughout the entire cross-section of each billet in the melt. ASTM E112, ASTM E1382, and the Russian standard GOST 21073 regulate approaches to grain size measurement. Currently, production laboratories primarily use an express method to analyse grain size. This method involves applying linear or circular secants of a known length to images of the grain structure. Then, the number of grain boundaries intersected by these secants is counted [2–4], as shown in Figure 1(c). The average conventional grain size, determined by this method, is the ratio of secant length to intersection count.

Following the high-temperature homogenization of billets, the supersaturated hydrogen solid solution decomposes and redistributes within the metal. This results in secondary microporosity along grain boundaries and dendritic cells, as illustrated in Figure 1(d), which is assessed during microstructure study. The presence of porosity primarily depends on the initial hydrogen content and is usually not observed in the microstructure when the content is less than 0.2 $cm^3/100$ g [1, 8]. Secondary microporosity is also affected by the temperature and duration of homogenization. The primary method of assessing porosity involves measuring its volume fraction in the microstructure using an image analysis software and classifying it accordingly. In the absence of an image analysis program, it is permissible to assign a porosity class by comparing the observed structure to reference scales.

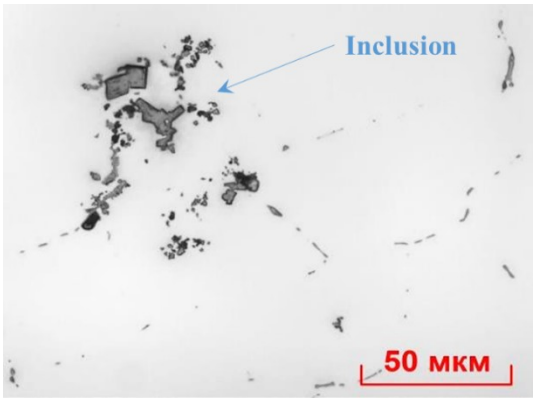

a) Inclusion

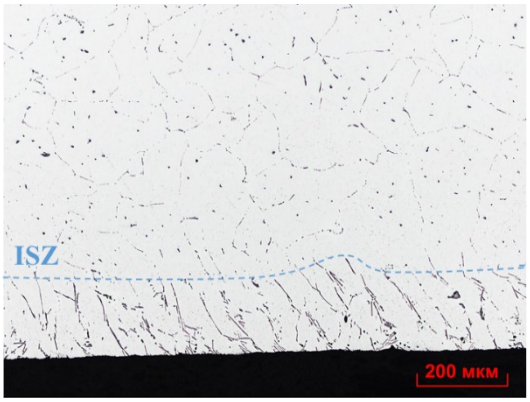

(b) Inverse segregation zone (ISZ)

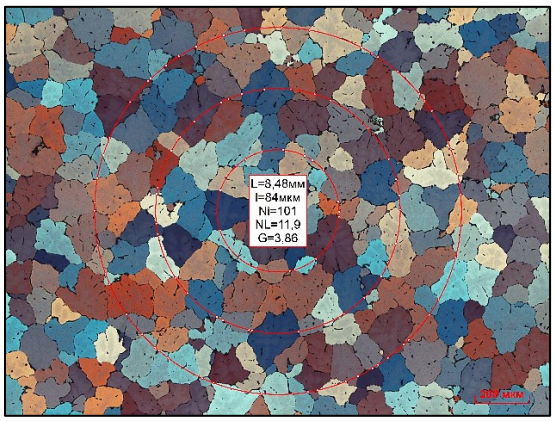

(c) Grains

(d) Secondary microporosity

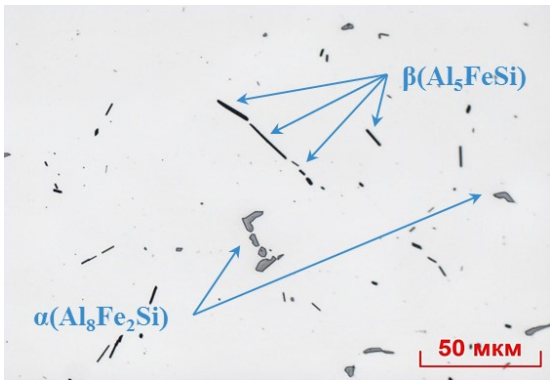

(e) AlFeSi particles

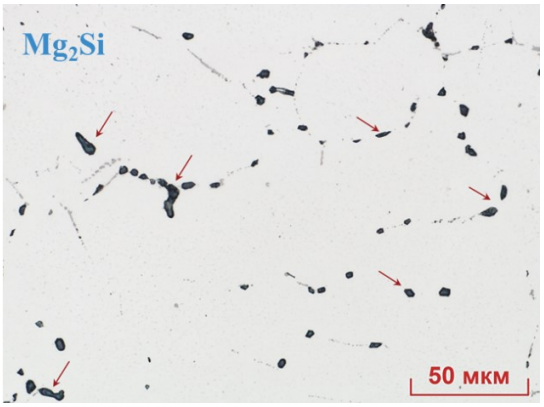

(f) Mg_2Si particles

Figure 1. Typical objects of analysis in 6xxx billet microstructure.

The presence of iron and silicon in 6xxx series alloys leads to the formation of iron-containing particles with different morphologies and compositions during crystallization. In alloys such as 6060, 6063, and 6005, the α(Al_8Fe_2Si) phase with favourable skeletal morphology and the β(Al_5FeSi)-phase with unfavourable lamellar morphology (acicular in the plane of the microsection) form during crystallization [1, 5, 6, 8, 12]. In alloys with higher manganese and chromium content, such as 6061 and 6082, the α($Al_{15}(Fe, Mn, Cr)_3Si_2$)-phase forms in a font-like

shape [1, 5, 6]. To improve the cast structure and enhance the technological properties, billets undergo homogenization, which reduces the negative impact of the unfavourable lamellar β(Al_5FeSi)-phase by transforming it into the favourable α(Al_8Fe_2Si)-phase and fragmenting all iron-containing particles. The production goal is to achieve a high degree of transformation and fragmentation of iron-containing phase particles. The degree of transformation is estimated by the ratio of α- and β-phase particles in the microstructure. This ratio can be determined after special etching, as shown in Figure 1(e). The criterion for fragmentation degree is the size of iron-containing phase particles [7]. A lab metallographer uses an image analysis program to analyse the number and size of iron-containing phase particles in a fixed area of the microsection.

In the structure of as-cast billets of 6xxx series alloys, the main alloying elements, magnesium and silicon, exist in solid solution and in the form of Mg_2Si particles located along grain boundaries and dendrites [1, 9]. To improve the billets' extrudability and obtain the profiles' required mechanical properties, the Mg_2Si particles must dissolve during homogenization and precipitate throughout the grains and dendritic cells in the form of dispersed secondary Mg_2Si particles during regulated cooling. Subsequently, the particles must dissolve easily under the action of extrusion temperatures and plastic deformation, which prepares the structure for solution heat treatment on the extrusion table. The cooling rate of the billets after high-temperature holding should produce a structure with a minimum amount or absence of Mg_2Si particles along the grain boundaries and dendritic cells and dense precipitation of particles throughout their bodies.

During microstructure analysis, the lab metallographer evaluates the number of Mg_2Si phase particles per unit area and the distribution type of the secondary particles, as shown in Figure 1(f). As with the evaluation of iron-containing phases, image analysis software is used.

RUSAL produces billets for domestic and foreign markets at five of its aluminum plants: KrAZ (Krasnoyarsk), VgAZ (Volgograd), SAZ (Sayanogorsk), NkAZ (Novokuznetsk), and TaAZ (Taishet). Each plant carries out serial quality control of the microstructure of the produced billets.

1.2 Limitations of Current Microstructure Analysis Approach

On average, analysing the microstructure of one sample with manual control takes four to five hours. Using image analysis programs with automated methods takes one to two hours.

Although image analysis software is available, some manufacturers still use complete manual analysis, which is a conservative and extremely labor-intensive process. Figure 2 shows an example of manually counting the number of α(Al_8Fe_2Si) and β(Al_5FeSi) iron-containing particles in one field of view to assess the degree of transformation. A laboratory metallographer observes the microstructure through a microscope's eyepieces and counts the number of particles of both phases. This process is repeated for each field of view until the desired number of results is achieved. This analysis procedure is repeated for all other microstructure parameters. Depending on the parameter, the number of analysed fields of view can range from 5 to 20. This approach is extremely ineffective and highly dependent on the qualifications of the specialist, as well as subject to significant human error.

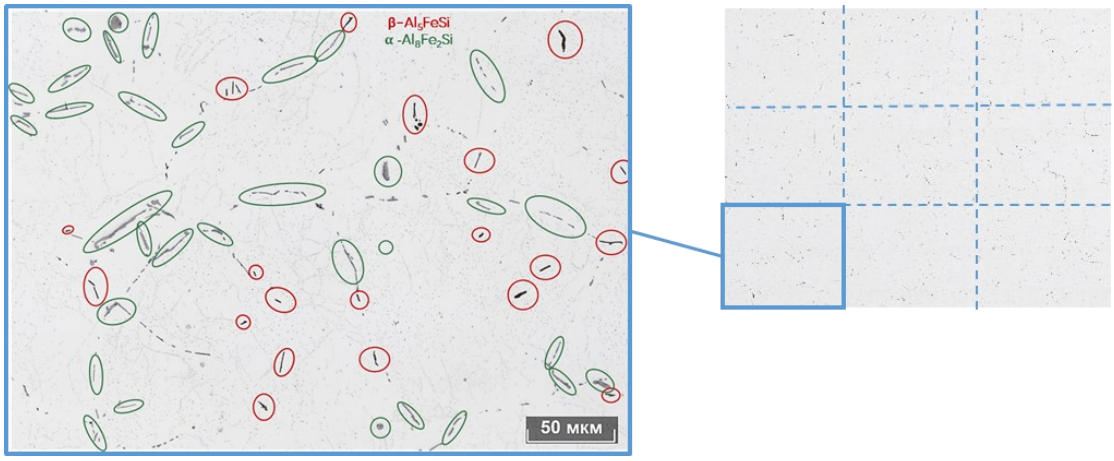

Figure 2. The ratio of one field of view to the total area of analysis for one microstructure parameter.

Image analysis software is the main tool for qualitative and quantitative microstructure analysis today. Using image analysis tools and automatic calculations open the possibility of using metrics that cannot be effectively used in manual analysis. For example, it allows one to calculate the volume fraction of microstructure objects. Additionally, it automates procedures and increases the speed of analysis.

This approach involves capturing microstructure images with a microscope camera. This makes it possible to select objects for analysis using a brightness histogram (gray level), as shown in Figure 3, or other criteria. Image analysis tools allow for the quantitative evaluation of various geometric and stereometric parameters of the selected objects.

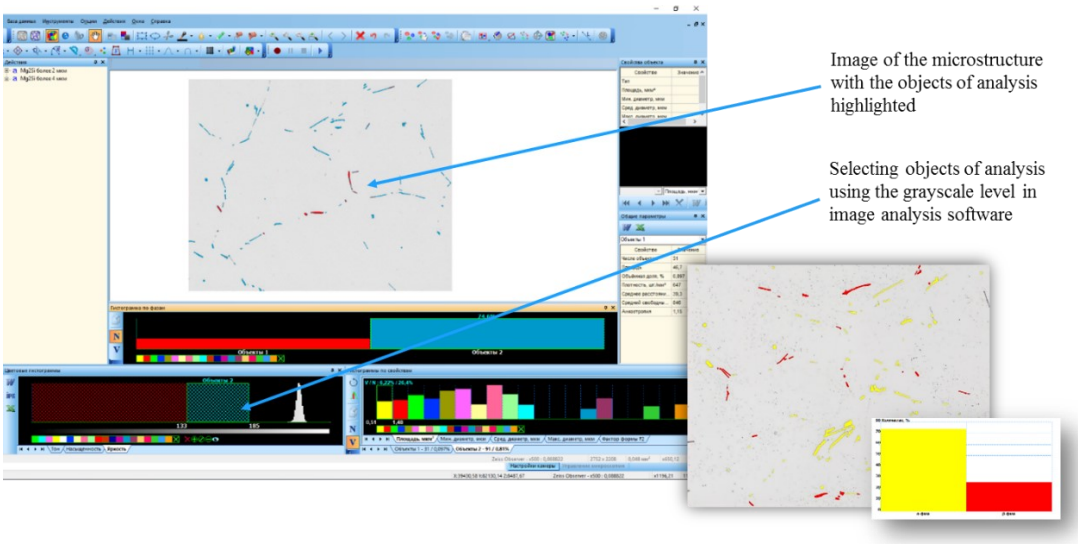

Figure 3. Microstructure analysis in image analysis software.

Image analysis software has long been the main tool used in industry for metallographic analysis. However, as modern methods were introduced, it became clear that these programs had limitations. They did not completely eliminate manual procedures or operator influence on the results. Despite the presence of automated tools in the software to facilitate routine tasks and improve quality of results, this remains specialized software that has a learning curve and requires

a certain level of qualification of the operator. Even in software, complex analysis of the microstructure is labour-intensive and time-consuming.

The approach to highlighting objects in the microstructure image software greatly influences the outcome. As mentioned above, the analysis objects are usually filled with bright/gray level. This is shown in Image 4. Of course, there are rules for correctly filling objects and adjusting the image settings. However, as practice shows, despite using the same approaches, different operators can highlight the analysis objects differently, which significantly affects the analysis results.

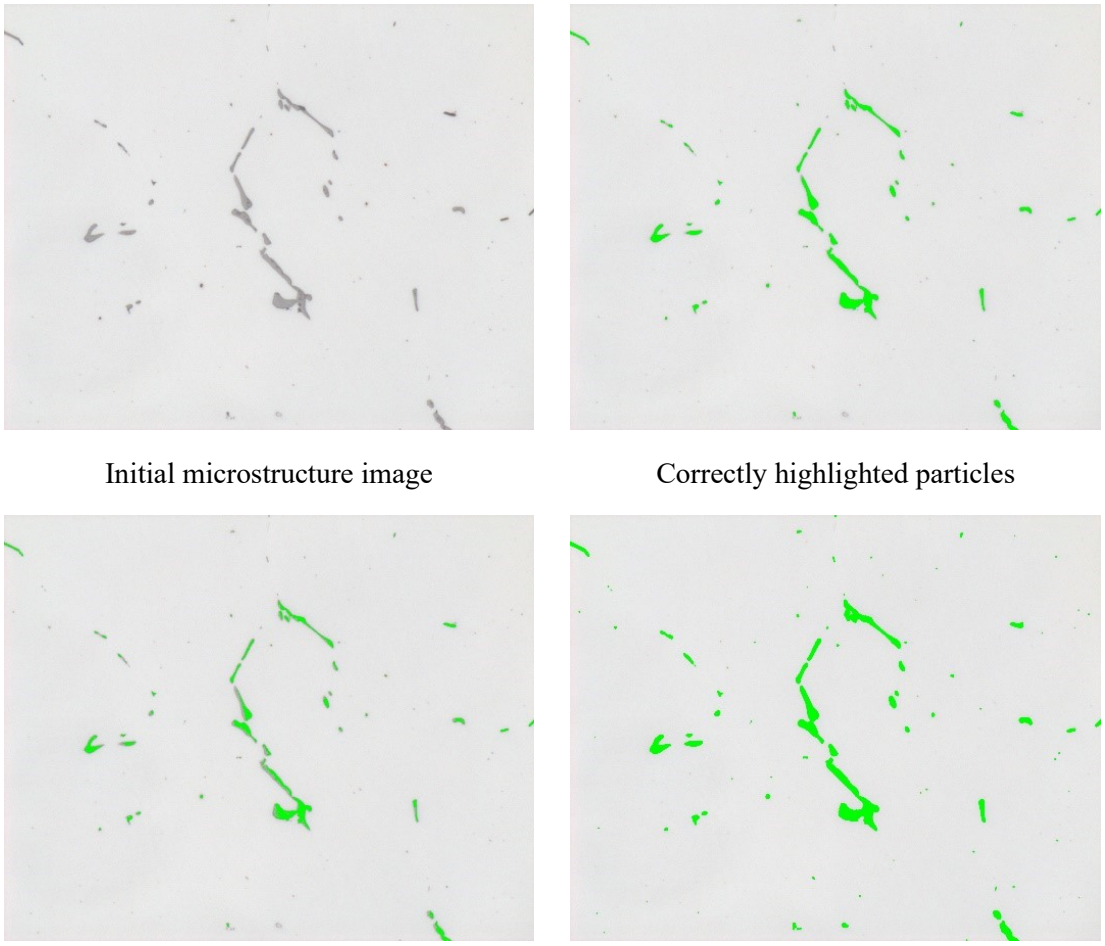

Initial microstructure image | Correctly highlighted particles

Insufficient particles highlighting | Excessively highlighted particles

Figure 4. Microstructure particles highlighted using image analysis software.

The results of the round-robin test, presented in Figure 5 as box plots, demonstrate this. The test examined four microstructure parameters: the number of Mg_2Si particles, the ISZ size, the degree of transformation of iron-containing phases, and the porosity class. Five metallographic laboratories participated in these tests, each analysing identical sets of images for each microstructure parameter using a single measurement technique. As can be seen, in some cases, the difference in results reached twice the amount, casting doubt on the reliability of the data obtained under reproducibility conditions, even when using image analysis programs and unified approaches. This also indicates a significant influence of the human factor.

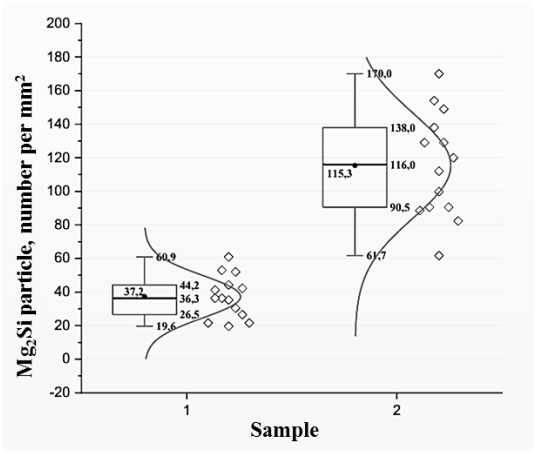

Number of Mg_2Si particles

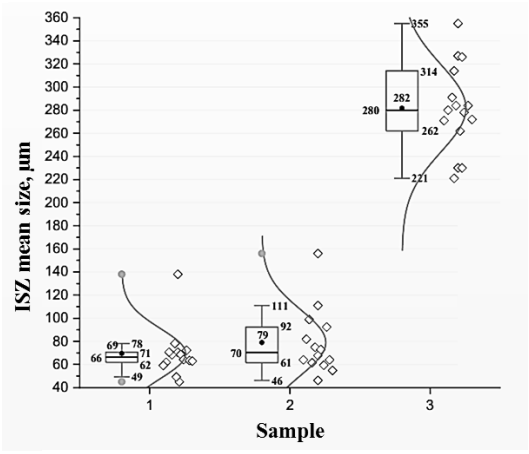

ISZ size

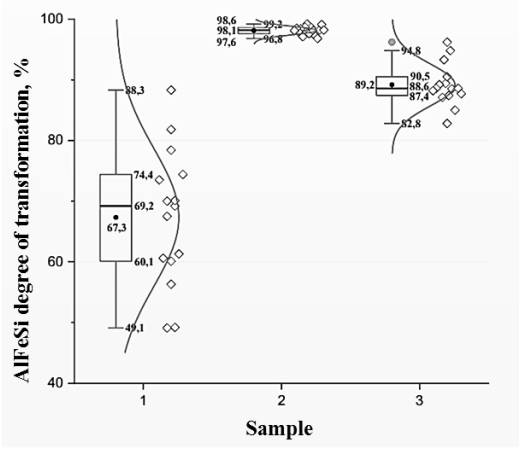

AlFeSi degree of transformation

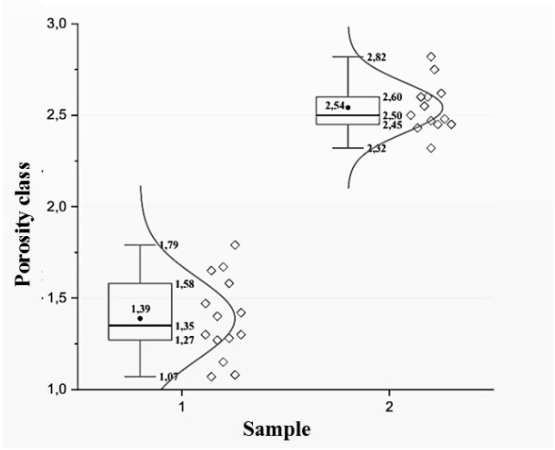

Porosity class

Figure 5. Results of round robin test.

1.3 In Search of Solution

We sought to automate microstructure analysis to reduce operator-dependent errors and improve efficiency. Initial efforts revealed that conventional methods struggled to address these needs effectively, as operator actions consistently introduced significant errors.

With AI and neural networks now accessible and widely adopted (e.g., in medical imaging and defect detection), we explored computer vision for this purpose. Collaborative market analysis with RUSAL's Digital Solutions team found no suitable off-the-shelf solutions tailored to our specific requirements.

A decision was made in conjunction with the Department of Production Automation of the ETC, which has specialists in machine vision, image analysis, and deep learning/neural network models, to develop a system for automatically analysing the microstructure of 6xxx series extrusion billets. This system would allow for fully automated analysis, eliminating the need for human involvement.

2. Building of Automatic Microstructure Analysis System (AMAS)

It took about 10 months to develop the first version of the Automatic Microstructure Analysis System (AMAS). The developed analysis system is complex software consisting of the following modules (Figure 6):

1. The image analysis service is deployed on the server. This service automatically analyses incoming microstructure images in batches using computer vision technologies and neural network models. It allows for the analysis of the main parameters of 6xxx series alloy microstructures according to the RAM-ST-2.6-25 method without operator intervention.
2. The desktop application allows for primary analysis settings, such as calibration and magnification. It automatically sends images from a selected directory to the server for analysis. The application calculates the rating score for each analysed microstructure parameter using the RAM-M-2.6-12 method. A score is assigned to each microstructure characteristic depending on the alloy and billet diameter. The application also generates a report of the results.
3. A system for automatically capturing a series of images, implemented by the developers of the microscope software. When selecting the initial coordinates on the microsection, this system allows to automatically capture the required number of images for analysis.
4. A web interface allows to check the accuracy of object identification in microstructure images and to perform expert control for the purpose of further analysis models training.

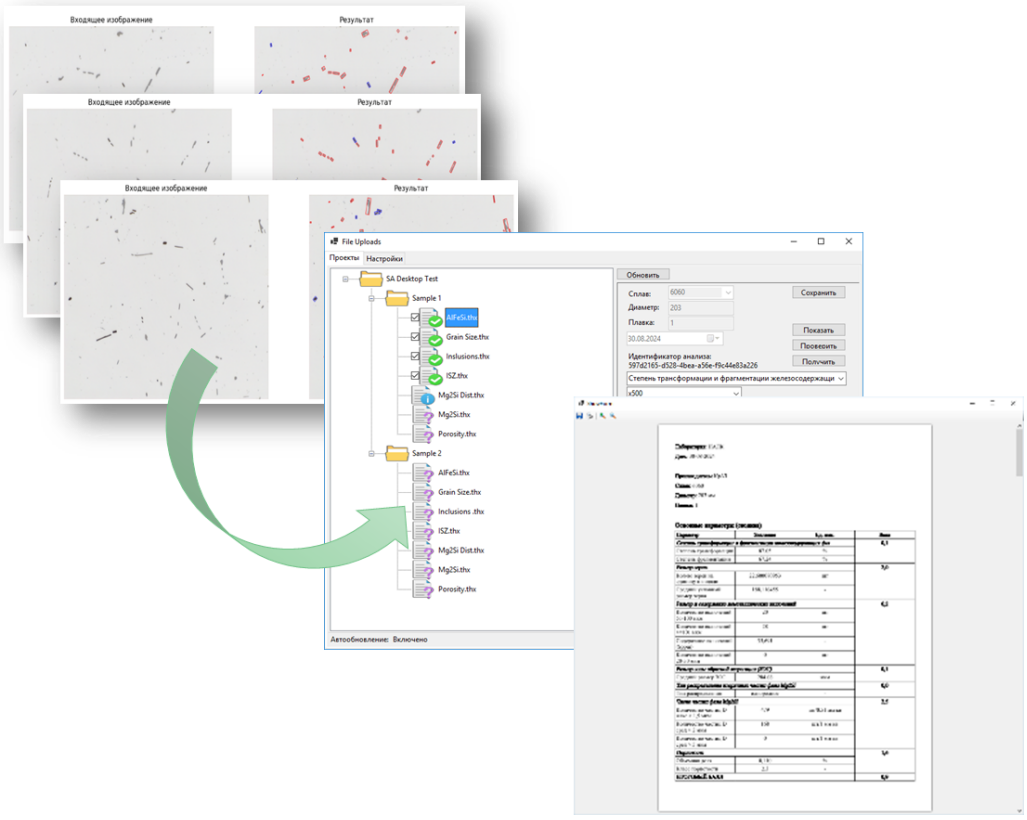

Figure 6. Batch image analysis, rating and report output in AMAS.

Table 2 shows the architecture of the analysis models underlying the image analysis service. The OpenCV library was used to analyse the degree of transformation/fragmentation of iron-containing phases, porosity, and the number of Mg_2Si phase particles. It is quick and easy to use and does not require a large amount of computing resources. The algorithms used include

mathematical algorithms of computer vision for finding boundaries and contours and algorithms for finding the smallest figures circumscribed around the found objects by area.

The capabilities of the OpenCV algorithms and models were insufficient for all the analysis parameters. For the remaining parameters, other approaches were necessary. One significant issue was the size of the input images, which were 275 2× 2208 pixels. The high resolution prevented processing in its original form. However, the target objects in the images are quite small. Therefore, any transformations associated with reducing the resolution resulted in the loss of important information and incorrect analysis results.

The U-Net architecture is often used for precise image segmentation, which requires extracting features pixel by pixel. First, the network successively reduces the image resolution by extracting important features. Then, it restores the image to its original size by combining the extracted features with spatial information from the initial layers. It is named after its U-shaped structure, which reduces training time due to connected layers. To solve our problems, we applied the technology of cutting the original image into smaller segments. The resulting packet is then sent to a modified U-Net with 32 filters on the first convolutional layer and a «softmax» activation function on the last convolutional layer. Next, the results of the packet are assembled in reverse order to resemble the original large image. We programmed our own neural networks in TensorFlow Keras and use them only where OpenCV algorithms are insufficient.

Table 2. Image processing service architecture

Microstructure parameter	Architecture
Number and size of inclusions	OpenCV and (development still in progress)
Inverse segregation zone size	Modified U-net
Grain size	Modified U-net
Porosity volume fraction and size	OpenCV
Degree of transformation and fragmentation of AlFeSi-particles	OpenCV
Number of Mg2Si particles	OpenCV
Distribution type of secondary Mg_2Si particles	Modified U-net

The biggest challenge was the small size of the training model datasets. We used image augmentation algorithms to solve this problem.

3. Current AMAS Performance

To test AMAS under real conditions, we selected collections of microsections with different values of the main measured parameters and types of microstructures for analysis. The samples were regularly analysed using both the existing microscope software and AMAS.

The following factors influenced the results of the parameter measurements:
– heterogeneity of the microstructure of the samples, different fields of view selected by the operators.
– differences in microscope settings and post-processing of camera images used by different operators when analysing microsections.
– different settings and measurement operations during analysis in the microscope software selected by the operators; these settings and operations include: brightness level (grayscale) for selecting analysis objects, brightness thresholds for separating analysis objects, settings for particle size screening and automatic identification of artifacts, settings for reconstruction and separation of grains structure.

Three highly qualified operators performed two parallel measurements of each parameter in both AMAS and Microscope software. After each measurement was taken, a photograph of the actual time was taken for each analysed parameter.

Since microstructure analysis is a standard-free method, a comparison of the statistical indicators of the AMAS and microscope measurements was carried out to evaluate the results. Box plots were constructed to visually present the results.

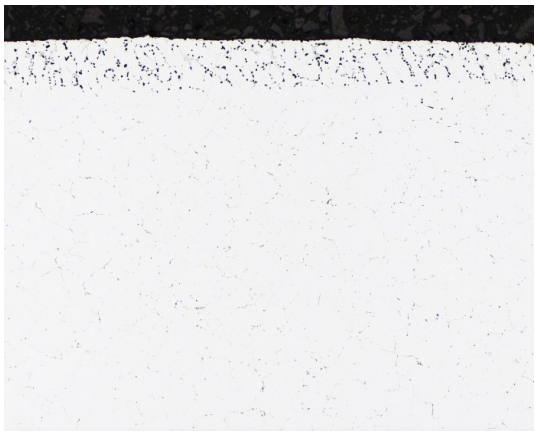

Initial image

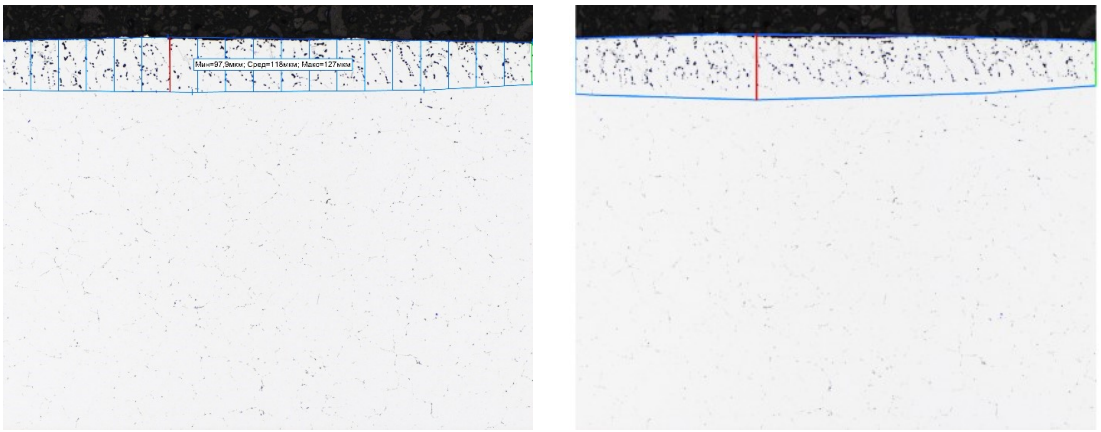

Image analysis software AMAS

Figure 7. ISZ detection comparison.

Figure 7 shows an example of ISZ identification in the microstructure of samples using microscope software and AMAS. Figure 8 presents the results of the analysis. Upon analysing the samples, we found that the current neural network model for identifying ISZs overestimates their values in many scenarios. While the automatic analysis system correctly recognizes the ISZ region at the boundary of the microsection, it is overly sensitive when determining the lower boundary, particularly in cases involving liquation peaks and local image inhomogeneities. Nevertheless, the results indicate that AMAS reliably measures ISZ size. Increasing the dataset for training will further improve the accuracy of the neural network model for analysing the ISZ.

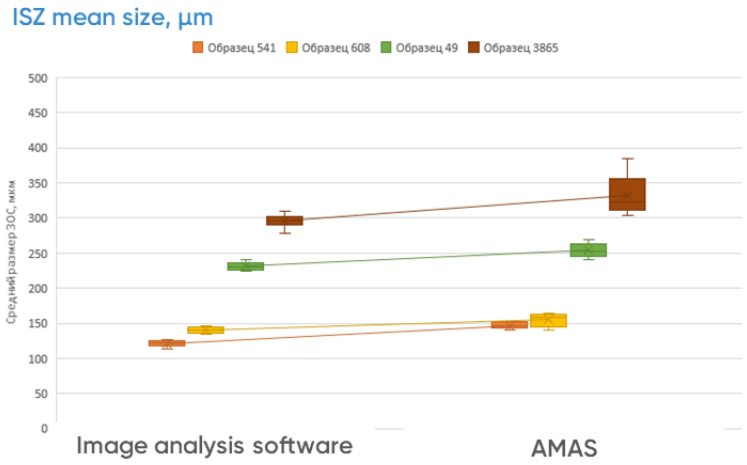

Figure 8. ISZ mean size analysis results comparison.

Figure 9 shows an example of grain identification in the microstructure of samples using microscope software and AMAS.

Figure 10 presents the analysis results. During analysis with the microscope software, operators noted the number of grain boundary intersections on secants superimposed on the image. The AMAS analysis model operates on the principle of detecting individual whole and boundary grains, and then converting the obtained value to the average conventional grain size using the extrapolation method. AMAS provided results identical to those obtained in the microscope software during the grain size analysis. The difference in the average conventional grain size values in all analysed samples did not exceed 4%. The neural network grain identification model, which is trained to work with grain structure images obtained using various types of polarizers, has proven effective.

Figure 11 shows an example of porosity identification in the microstructure of samples using microscope software and AMAS.

Figure 12 presents the analysis results. The analysis system accurately identified secondary porosity in all tested scenarios. The pores volume fraction values obtained using the analysis system and the microscope software are nearly identical.

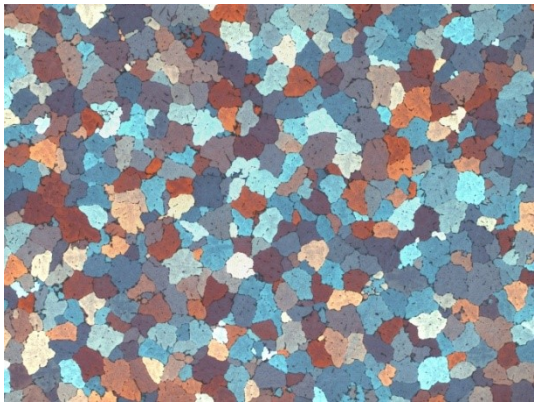

Initial image

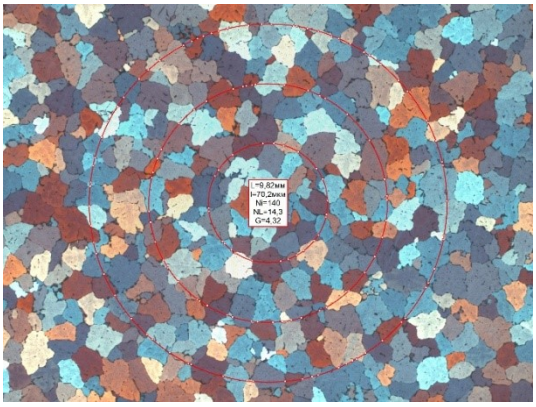

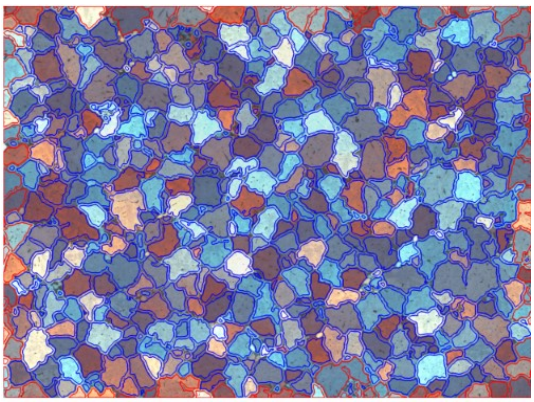

Image analysis software AMAS

Figure 9. Grains detection comparison.

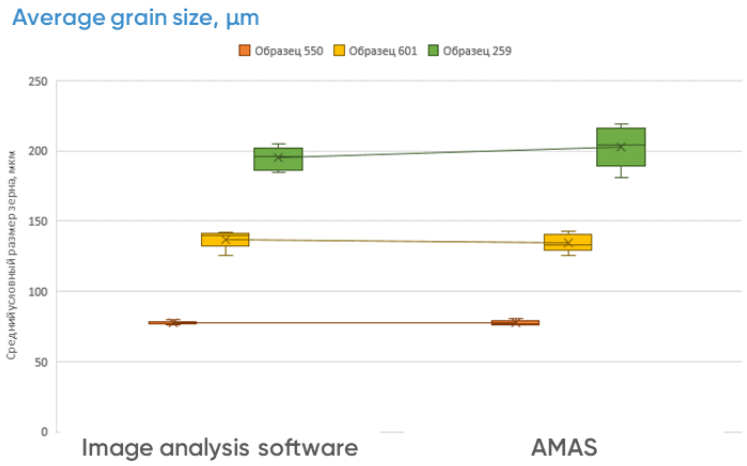

Figure 10. Mean grain size analysis results comparison.

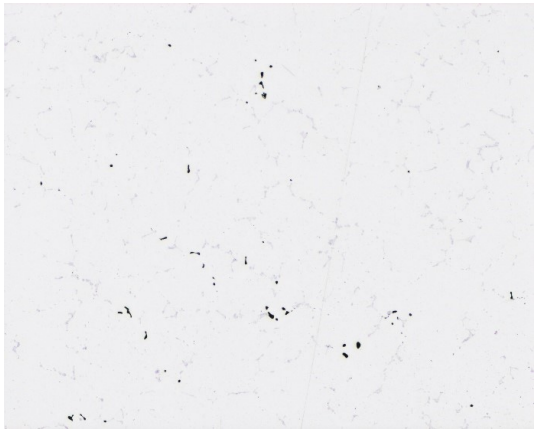

Initial image

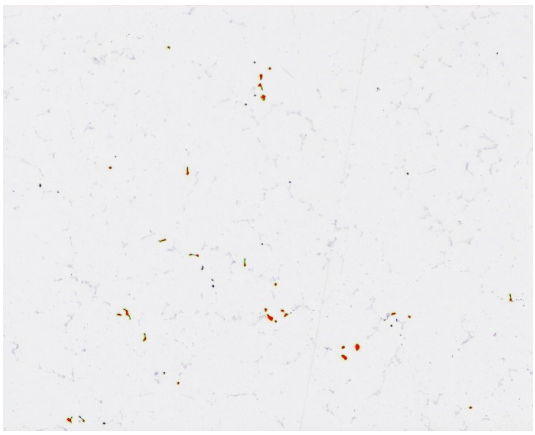

Image analysis software AMAS

Figure 11. Porosity detection comparison.

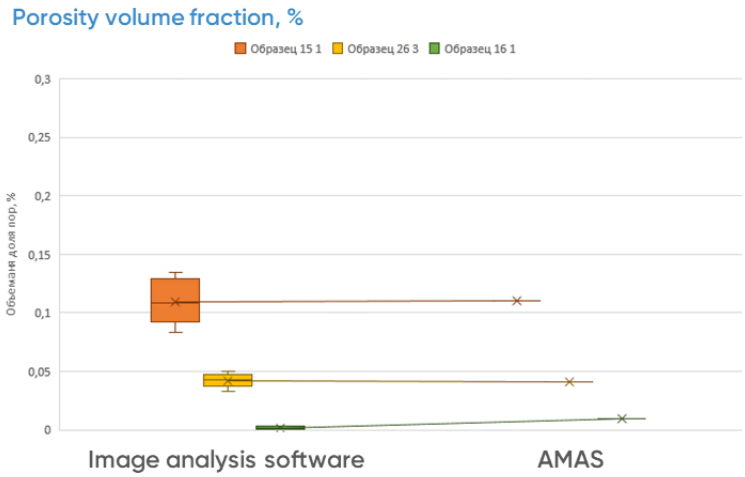

Figure 12. Porosity volume fraction analysis results comparison.

Figure 13 shows an example of the identification of α(Al_8Fe_2Si) and β(Al_5FeSi) iron-containing phases during the analysis of transformation degree in samples using microscope software and AMAS.

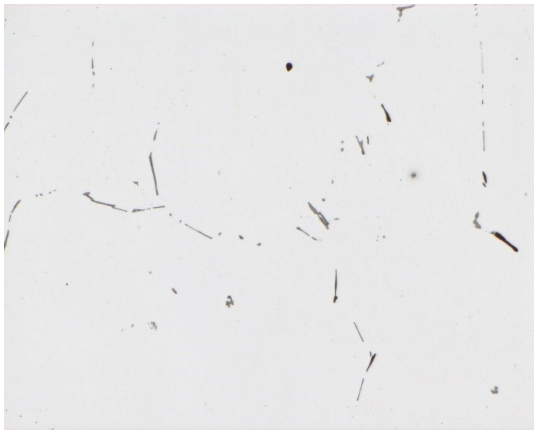

Initial image

Image analysis software

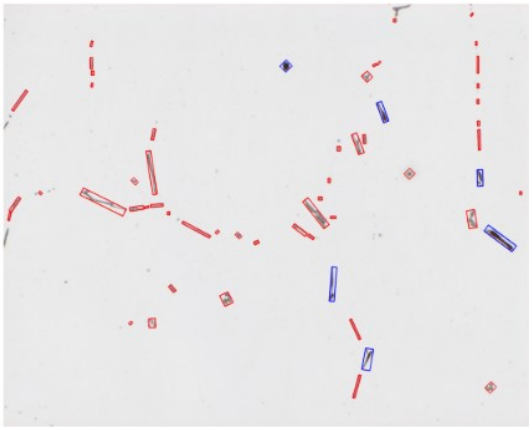

AMAS

Figure 13. α(Al_8Fe_2Si) and β(Al_5FeSi) particles detection comparison.

Testing results showed that AMAS provides satisfactory comparability with microscope software when analysing samples with a transformation degree greater than 70%. This degree of transformation is sufficient for most serial microstructure control analysis scenarios, even though AMAS slightly underestimates the final transformation degree value. When analysing samples with a low transformation degree, significant variation in the obtained values is observed in both the microscope software and the AMAS. This indicates significant sample heterogeneity and error in this measurement range. On average, AMAS overestimates transformation degree values compared to the microscope software in this range because many β-phase particles with irregular morphology are identified as α-phase particles. To operate AMAS more accurately in this measurement range, the analysis model may require additional adjustment.

When analysing the degree of fragmentation, AMAS provides results that are identical to those obtained using microscope software. The difference in final fragmentation values between instruments does not exceed 3 %.

Figure 14(a) shows the results of the transformation degree analysis, and Figure 14(b) shows the fragmentation degree.

Figure 15 shows an example of identifying Mg_2Si phase particles in the microstructure of samples using microscope software and AMAS. Figure 16 shows the analysis results. In most scenarios,

AMAS provides results comparable to those obtained using the microscope software when analysing samples.

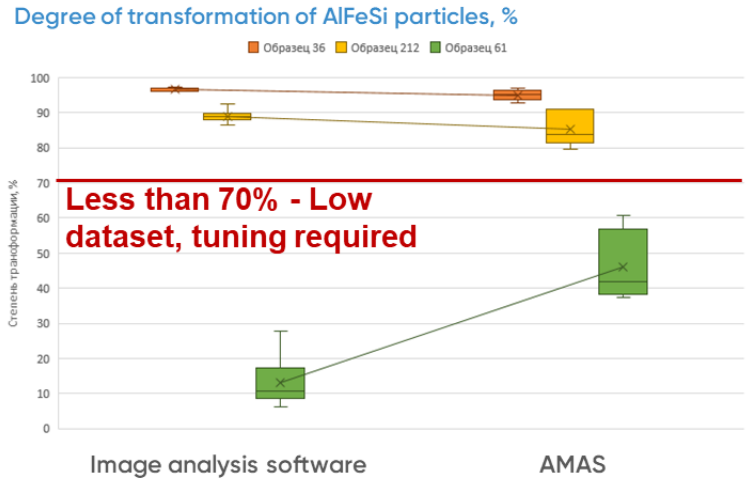

a

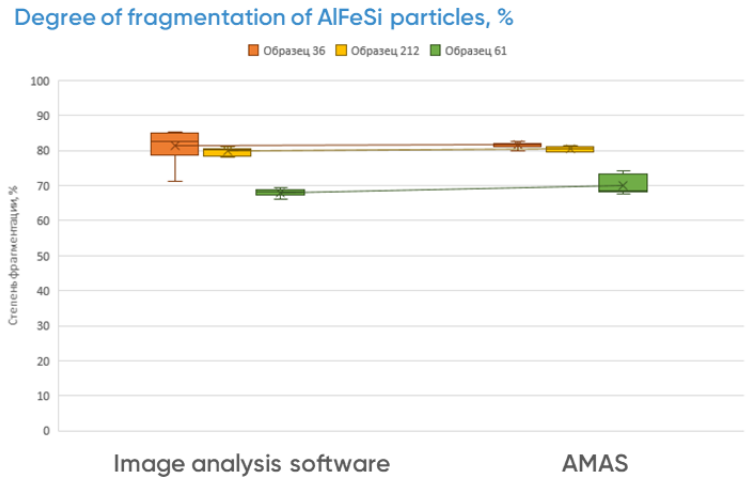

b

Figure 14. Degree of transformation (a) and fragmentation (b) of AlFeSi particles analysis results comparison.

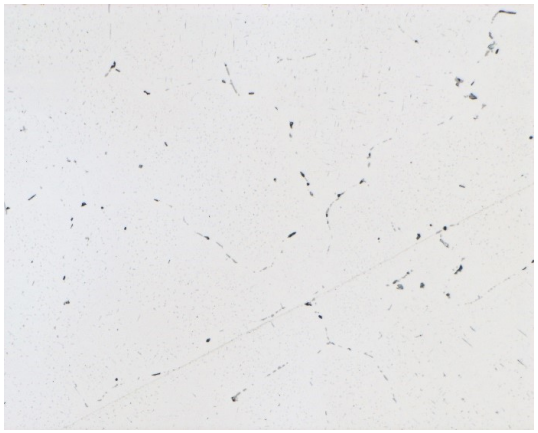

Initial image

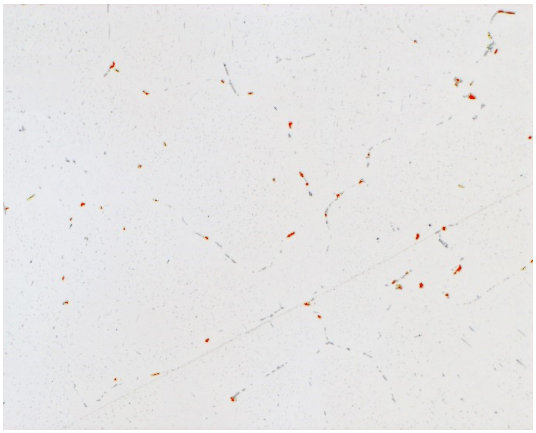

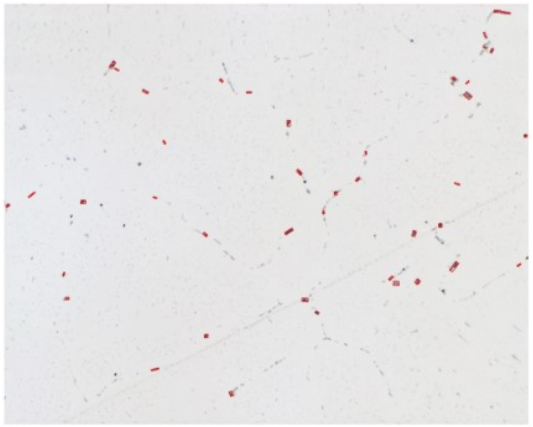

Image analysis software AMAS

Figure 15. Mg_2Si particles detection comparison.

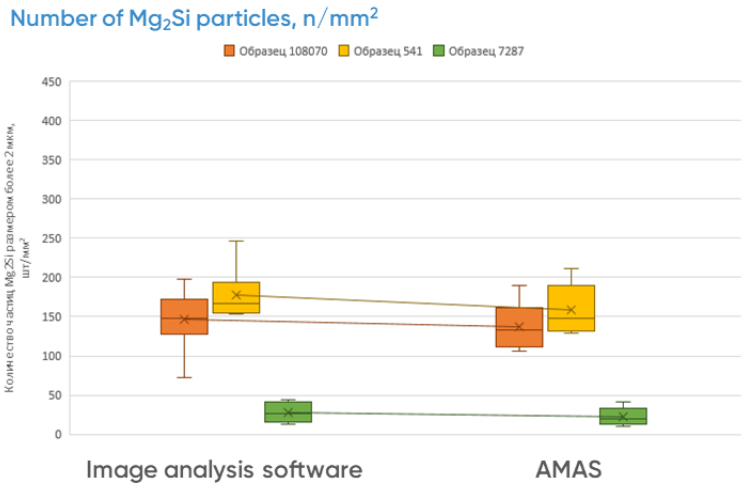

Figure 16. Number of Mg_2Si particles analysis results comparison.

Currently, AMAS is trained to recognize three types of Mg_2Si phase secondary particle distribution: homogeneous, depleted, and segregated, as shown in Figure 17. When analysing 45

control images with these types of distributions, the correct result was obtained in approximately 70 % of cases. While the neural network model's accuracy for this indicator is not ideal, it is satisfactory for the system's further use in analysing this indicator under the user's control. Improving the accuracy of recognizing distribution types further can be achieved by increasing the dataset for training the neural network model more.

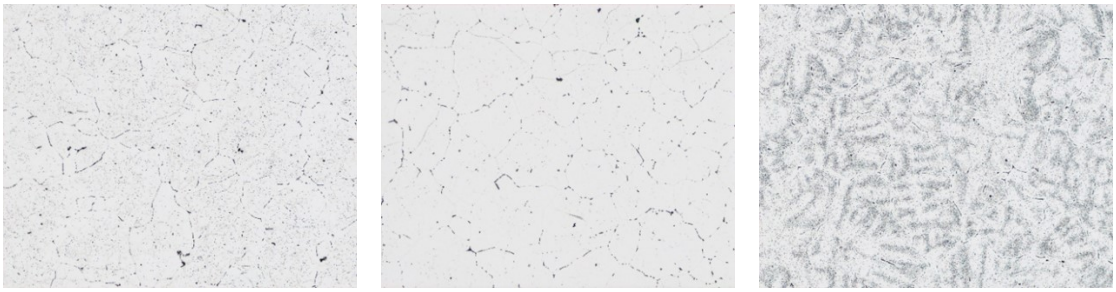

Even/homogenous **Poor/depleted** **Segregation**

Figure 17. Secondary Mg_2Si particles distribution types detection using AMAS.

The current version of AMAS correctly identifies inclusions in the structure but often misidentifies their boundaries, particularly in the case of inclusion clusters (see Figure 18). Additionally, some structural components of the alloy, such as irregularly shaped iron-containing phase particles, are often misidentified as inclusions.

Various approaches and algorithms were used to solve the inclusion identification problem, but training a neural network model to recognize inclusions in the aluminium microstructure showed the greatest potential efficiency. In 2024, TMS Light Metals published three articles on the possibility of using AI machine learning technologies for the PoDFA automation method [26–28], which indicates good potential of this approach.

As of this writing, the dataset for effectively training the neural network model is still being collected. This is because, unlike the structural components of the alloy, inclusions can have different morphologies, types, sizes, and colours, making them difficult to identify in the structure.

In order to implement an effective solution, it is necessary to continuously collect a dataset consisting of labelled images of various types of inclusions in aluminium microstructures. Further training of the neural network model is also required to achieve the necessary level of accuracy. Additionally, developing a universal model for recognizing inclusions in various aluminium alloys could solve this problem and allow for faster collection of a dataset for effectively training the analysis model.

4. Efficiency of AMAS

AMAS with an average control volume of 25 billet samples per month is four times faster than analysing samples with specialized software, and eleven times faster, compared to manual measurement.

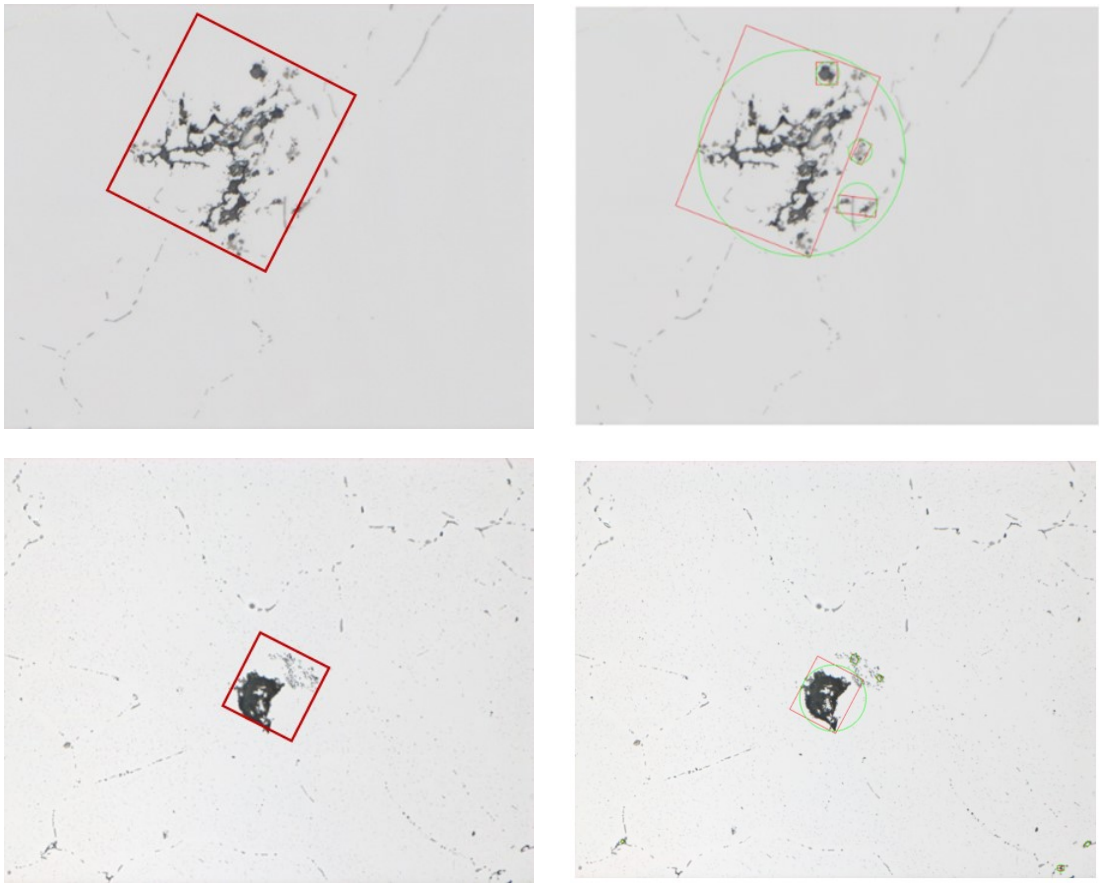

Required Identification **Identification in AMAS**

Figure 18. Inclusions detection examples using AMAS.

Table 3. Analysis duration using different methods

Microstructure parameter	**Manual measurement**	**Software for image analysis**	**AMAS***
	minutes		
Number and size of inclusions	60	15–30	9–15
Inverse segregation zone size	30–40	10–20	1–2
Grain size	30–40	10–20	1–2
Porosity volume fraction and size	40–60	15	1–2
Degree of transformation and fragmentation of AlFeSi-particles	40	5–10	1–2
Number of Mg_2Si particles	30–40	10	1–2
Distribution type of secondary Mg_2Si particles	5–10	5–10	1–2
TOTAL for sample	**4–5 hours**	**1 h 10 min–2 hours**	**15–27 minutes**

*According to data received from ETC Scientific and Analytical: The actual analysis time depends on PC speed and network connection and may vary among users. These factors influence the speed at which microstructure images are transferred to the server and responses are received.

5. Initial Role Out and Next Steps

Since the beginning of 2025, AMAS has operated on RUSAL ETC's central server, where a powerful video card is the main component for operating and training analysis models. AMAS is currently undergoing industrial testing and is being used for quality control of the microstructure of 6xxx series alloy billets, running in parallel with the current microscope software analysis.

AMAS is expected to launch at all five RUSAL billet producing plants in 2025–2026. The existing server capacity is expected to meet the needs of all the company's laboratories. However, the computing power required is still to be demonstrated.

6. Conclusions and Learnings

The developed system of automatic microstructure analysis (AMAS) for 6xxx series extrusion billets is comprehensive software that uses computer vision technologies and neural network models to automatically survey and analyse microstructure parameters without operator participation. This system completely eliminates the influence of the human factor on the result.

Using the developed AMAS significantly reduces the time needed to analyse key microstructure parameters of 6xxx series billets and ensures results comparable to those obtained by operators using image analysis software in most scenarios.

The results obtained indicate the viability and potential of unattended microstructural analysis using AMAS. The accuracy of AMAS improves with an increased dataset for training neural network analysis models.

7. Possible Risks

While AMAS analysis models are fully functional (excluding inclusion analysis) and deliver satisfactory lab results, their performance on plant laboratory equipment still requires validation. Adaptation during implementation may be necessary to ensure compatibility across diverse operating conditions.

8. References

1. G.S. Makarov, Billets made of aluminium alloys with magnesium and silicon for extrusion, *Production Fundamentals*, Moscow: Intermet Engineering, 2011, 528 p.
2. ASTM E112-2013, Standard test methods for determining average grain size.
3. ASTM E1382-1997 (R 2015), Standard test methods for determining average grain size using semiautomatic and automatic image analysis.
4. GOST 21073.3-75, Non-ferrous metals. Determination of grain size by the method of counting grain intersections.
5. N.C.W. Kuijpers, Kinetics of the β-AlFeSi to α-Al(FeMn) Si transformation in Al-Mg-Si alloys, *PROEFSCHRIFT*, 2004.
6. Niels C. W. Kuijpers, Fred J. Vermolen, Kees Vuik, Sybrand van der Zwaag, A model of the -AlFeSi to -Al(FeMn)Si transformation in Al–Mg–Si alloys, *Materials Transactions*, Vol. 44, No. 7, 2003, 1448-1456.

7. Jostein Røyset, Øystein Bauger, Jan Anders Sæter, Ulf Tundal, Oddvin Reiso, Homogenization of Al-Mg-Si alloy billets – myths and facts, *ET 2012 Proceedings*, Volume 2, 171-185.
8. María Victoria Canullo, Rodolfo Acuña Laje, Metallurgical quality of Aluar billets, ten years of increasing quality, *ET 2008 Proceedings*, Volume 2, 43-57.
9. J.D. Schloz, Advanced 6xxx alloys – challenges in casting and extrusion process, *ET 2008 Proceedings*, Volume 2, 181-203.
10. AI MSE 2025, https://dgm.de/aimse/2025 (Accessed on 26 May 2025).
11. Lisa Sweet, Xinquan Zhang, Nick Birbilis, Mark A. Easton, The influence of iron content on the tensile properties and anodizing response of AA 6060 extrusions, *ET 2012 Proceedings*, Volume 2, 1-11.
12. Malcolm J. Couper, Elizabeth D. Sweet, Xinquan Zhang, Influence of Fe and Mn content on 6xxx extrusion alloys, *ET 2012 Proceedings*, Volume 2, 35-42.
13. Oddvin Reiso, Martin Lefstad, Jostein Røyset, Ulf Tundal, Flow of billet surface material during extrusion of Al alloys; effect of billet quality and process conditions, *ET 2012 Proceedings*, Volume 1, 33-48.
14. Jostein Røyset, Øystein Bauger, Oddvin Reiso, Ulf Tundal, Innovations in billet casting and homogenization, *ET 2016 Proceedings*, Volume 2, 1-16.
15. Tony Da Silva, Blisters and their many causes, *ET 2016 Proceedings*, Volume 2, 221-238.
16. G. Liu, L. Zhou, J. Luo, Effect of Fe-rich intermetallic phases on the extrusion behavior of 6xxx series aluminum alloys, *Journal of Materials Processing Technology*, 255, 2018, 749-757.
17. R. Zhang, Z. Zheng, Y. Li, Influence of AlFeSi phase morphology on the hot deformation behavior and extrusion speed of 6063 aluminum alloy, *Journal of Alloys and Compounds*, 688, 2016, 712-720.
18. O. Reiso, Extrusion of 6xxx alloys with high Fe content, *Proceedings of the 8th International Aluminum Extrusion Technology Seminar (ET 2004)*.
19. G. Liu, G.J. Zhang, X.D. Ding, J. Sun, K.H. Chen, Modeling the strengthening response to aging process of Al-Mg-Si-Cu alloys, *Materials Science and Engineering: A*, 344(1-2), 2004, 113-124.
20. C.D. Marioara, S.J. Andersen, J. Jansen, H.W. Zandbergen, The influence of alloy composition on precipitates of the Al-Mg-Si system, *Acta Materialia*, 49(2), 2001, 321-328.
21. Y. Birol, Effect of homogenization practice on the microstructure of AA6063 billets, *Journal of Materials Processing Technology*, 186(1-3), 2007, 94-101.
22. P.K. Saha, Influence of precipitation hardening on extrusion of aluminum alloys, *Journal of Materials Engineering and Performance*, 9(5), 2000, 516-524.
23. W. Liang, P.A. Rometsch, L.F. Cao, Effects of aging treatment on the mechanical properties and extrudability of Al-Mg-Si alloys, *Materials Science and Engineering: A*, 532, 2012, 548-557.
24. William Dixon, Extrusion surface effects resulting from billet surface inflow, *Proceedings of the 9th International Aluminum Extrusion Technology Seminar (ET 2008)*, Volume 1, 245-260.
25. Richard M. Kelly, Paul F. Chaveriat, Kelly P. Wardlow, Steven R. Claves, Wojciech Z. Misiolek, Predictive metallographic assessment of extrudability and comparative testing of 6xxx aluminum alloy billets, *Proceedings of the 8th International Aluminum Extrusion Technology Seminar (ET 2004)*, Volume 2, 39-50.
26. Hannes Zedel, Eystein Vada, Robert Fritzsch, Shahid Akhtar, Ragnhild E. Aune, Automated metal cleanliness analyser (AMCA): improving digital image analysis of PoDFA micrographs by combining deterministic image segmentation and unsupervised machine learning, *TMS Light Metals 2024 Conference Proceedings*.

27. Pascal Gauthier, Vincent Bilodeau, John Sosa, A PoDFA benchmarking study between manual and AI-supervised machine learning methods to evaluate inclusions in wrought and foundry aluminum alloys, *TMS Light Metals 2024 Conference Proceedings*.
28. Anish K. Nayak, Hannes Zedel, Shahid Akhtar, Robert Fritzsch, Ragnhild E. Aune, Enhancing quantification of inclusions in PoDFA micrographs through integration of deterministic and deep learning image analysis algorithms, *TMS Light Metals 2024 Conference Proceedings*.